

Effect of temperature on self-assembly of an ionic tetrapeptide

M. R. Tiné · M. Alderighi · C. Duce ·
L. Ghezzi · R. Solaro

AICAT2010 Special Chapter
© Akadémiai Kiadó, Budapest, Hungary 2010

Abstract The self-aggregation of the ionic tetrapeptide RWDW (R = arginine, W = tryptophan, D = aspartic acid) was studied at three temperatures (15, 25 and 35 °C) by different experimental techniques such as atomic force microscopy (AFM), isothermal titration calorimetry (ITC) and differential scanning calorimetry (DSC). AFM was used to investigate the morphology of the aggregates; the AFM images at 15 °C showed the presence of a dense network of entangled fibres, while at 35 °C the peptide assembled into sparse globular and fibrillar structures. Moreover, the calorimetric experiments showed that in all cases the disaggregation process is endothermic and dependent on the investigated temperature. Both the enthalpy of disaggregation and the ΔC_p change with temperature. In particular, at 35 °C, we obtained the lower enthalpy of disaggregation and higher ΔC_p , showing that the disaggregation process is favoured at high temperature. The DSC scans strengthen the hypothesis that the RWDW aggregation is a rather complex phenomenon.

Keywords Atomic force microscopy · Isothermal titration calorimetry · Oligopeptide · Self-assembly · Differential scanning calorimetry

Introduction

Molecular self-assembly has emerged as a powerful strategy in biomedical and pharmaceutical areas [1]. In particular,

peptide self-assembly has been extensively investigated, to study protein folding, to investigate protein conformational diseases [2–4] and as injectable scaffolds for the healing of damaged tissues in tissue engineering [5–8]. Among self-assembling peptides, the class of ionic complementary peptides is of special interest [9]. They have repeating units with positively and negatively charged residues separated by hydrophobic residues that allow the formation of complementary ionic pairs within each chain and/or between different chains.

Recently, we started an interdisciplinary study to explore the self-assembly of short ionic oligopeptides as both models of polypeptides and potential biomedical materials [10–12]. We investigated, in particular, the self-aggregation of 12 ionic oligopeptides constituted by 4–7 units and containing neutral and charged amino acid residues. We showed that the critical aggregation concentration (ΔC_p) of tetrapeptides decreases with increasing hydrophobicity of neutral residues. The dependence of the ΔC_p of isomeric oligopeptides on the distribution of amino acid residues confirmed the high tendency to self-organization of molecules with alternating ionic and neutral residues. Indeed, atomic force microscopy (AFM) images recorded on oligopeptide solutions above the ΔC_p showed the presence of either fibrillar or spherical aggregates depending on oligopeptide structure, concentration and time [10]. Moreover, the potential of the investigated oligopeptides in tissue engineering applications was supported by their low *in vitro* cytotoxicity [10] and by their ability to support cell adhesion and proliferation [12].

Recently, it has been discussed the role of temperature during self-assembly phenomena specially referring to temperature-induced gelation [13–15]. More recently, Ramachandran et al. [17] demonstrated that elevating the assembly temperature from 5 to 25 °C significantly changes

M. R. Tiné (✉) · M. Alderighi · C. Duce · L. Ghezzi ·
R. Solaro
Department of Chemistry and Industrial Chemistry, University
of Pisa, Via Risorgimento 35, 56126 Pisa, Italy
e-mail: mrt@dcci.unipi.it

the structure and mechanical properties of hydrogels formed by mutually complementary, self-repulsive oligopeptide pairs. On the other hand, Zhaoyang et al. [16] studied the self-assembly behaviour of RADA16-I using circular dichroism and AFM measurements in heat-denatured conditions, showing that the peptide, when heat-denatured from 25 to 70 °C, was still able to assume a typical β -sheet structure, but self-assembled into small-sized globular aggregates at much higher temperature.

Among the self-assembling oligopeptides that we previously studied, the RWDW tetrapeptide (R = arginine, W = tryptophan, D = aspartic acid) is of special interest because of its high tendency to self-organize [10, 11] and to form stable hydrogels in cell culture medium [12]. Therefore, in this study, we investigated further the RWDW self-assembly to assess the influence of temperature. In particular, isothermal titration calorimetry (ITC), differential scanning calorimetry (DSC) and AFM were used as complementary techniques to investigate the effect of assembling temperature on aggregation behaviour of RWDW in phosphate buffer solution. To this end, we selected three temperatures that can be easily achieved in a laboratory setting: 15, 25 and 35 °C.

Experimental

Materials

All reactants were analytical grade. Phosphate buffer (PB100; 100 mM, pH 3.5) was prepared by dissolution of 1.303 g of KH_2PO_4 in 100 mL of 0.042% H_3PO_4 . Phosphate buffer (PB50; 50 mM, pH 3.5) was obtained by 1:1 dilution of PB100. All aqueous solutions were prepared by using Milli-Q Advantage (Millipore, Bedford, MA, USA) water.

RWDW (>95% purity) was purchased from Advanced ChemTech (Louisville, KY, USA) and stored at -18 °C in sealed vials containing 10 mg sample. RWDW solutions in PB50 were obtained by dissolving a weighed amount of oligopeptide in water followed by the addition of an equal volume of PB100. Both water and PB100 were pre-equilibrated in a thermostatic bath at 15, 25 or 35 °C; the obtained peptide solutions were also thermostated at 15, 25 or 35 °C depending on the experiments and utilized at least after 2 h from the preparation to accomplish the aggregation phenomenon.

Peptide solutions for the DSC measurements were prepared by dilution of ITC solutions with PB50.

Methods

pH measurements were made using a combined glass microelectrode (Hamilton, Biotrode 238140/05) in

connection with an automatic Radiometer Analytical TIM 900 pH meter.

Isothermal titrations were performed by a Thermal Activity Monitor 2277 (Thermometric, Stockholm, Sweden), equipped with a 612 Lund syringe pump and a 4-mL ampoule. Aliquots of 50 or 100 μL of 1.5–2.0 mM thermostated tetrapeptide solutions in PB50 were repeatedly added to 2 mL of PB50 in 4 mL sample cell. The instrument was pre-equilibrated at 15, 25 or 35 °C depending on the experiments. Each titration was performed thrice to guarantee the reproducibility of the results.

DSC was performed on Nano-DSC III (TA Instruments, New Castle, DE, USA). Each scan was performed between 5 and 85 °C with heating and cooling rates of 1 °C/min. Before each series of experiments, the solution was degassed for about 15 min.

AFM measurements were performed by a multimode instruments connected to Nanoscope IV controller and equipped with E and J piezoelectric scanners (Veeco Instruments Inc., Plainview, NY, USA). The Thermal Applications Controller (Veeco Instruments) was used to maintain the samples at the selected temperature during scanning. Tapping mode scans were carried out by using silicon nitride RTESP (Veeco Instruments) and NSG01 (NT-MDT Co., Moscow, Russia) cantilevers having 40 and 5.5 N/m nominal elastic constant and 300 and 150 kHz resonance frequency, respectively. Samples for measurements in air were prepared by placing 10 μL oligopeptide solution in pH 3.5 of 50 mM phosphate buffer on freshly exfoliated muscovite mica. The peptide solution was kept for either 20 or 300 s on the mica surface, then washed with distilled water kept at the investigated temperature and finally dried with dry nitrogen flux. The dried sample was immediately inserted into the microscope head that was maintained at the selected temperature throughout the measurement time. Statistical analysis of AFM images was performed by Igor Pro 6.12 (WaveMetrics Inc., Lake Oswego, OR, USA).

Results and discussion

All experiments were performed at three different temperatures (15, 25 and 35 °C) to evaluate the effect of assembling temperature on the aggregation behaviour of RWDW and on the structure of oligopeptide aggregates.

Previously, we reported AFM images of RWDW solutions showing the formation of aggregates whose number and length increased with increasing oligopeptide concentration [10]. In this study, the concentration of oligopeptide solutions used for AFM imaging was 1.9 mM, a value well above RWDW cac (0.2–0.5 mM) [10].

RWDW topographic images recorded at 15, 25 and 35 °C after 20 s contact with mica (Fig. 1) show the presence of sparse fibrils whose number, width and height increase with increasing temperature (Table 1). On the other hand, the longest aggregates are formed at 25 °C. The observed trend indicates that the temperature somewhat affects the oligopeptide self-assembly. Still, the amount of mica surface covered by aggregates is almost constant at about 28%. Apparently, the contact time between the oligopeptide solution and the support is too short to allow a significant adhesion of aggregates independent of solution temperature. Accordingly, AFM measurements were repeated at the same

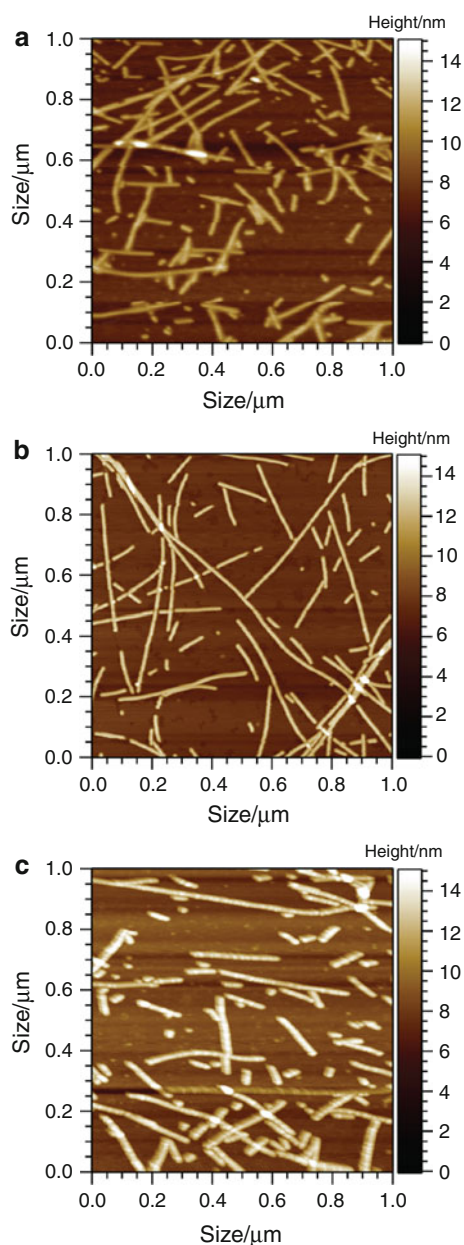


Fig. 1 AFM topographic image of RWDW 1.9 mM solution in PB50 cast on mica after 20 s contact time: **a** 15 °C, **b** 25 °C and **c** 35 °C

temperatures by increasing the contact time to 300 s (Fig. 2).

Topographic images of RWDW recorded at 15 °C indicate that 44% of the mica surface is covered by a rather dense network of entangled fibres (Fig. 2a). Images recorded at 25 °C (Fig. 2b) show the presence of a layer of fibrils (31% coverage) on top of a second layer of fibrils (98% total coverage). The fibril entanglement does not allow for measuring the length of fibres. It seems however that RWDW self-assembly gives rise to shorter and thicker aggregates at this temperature. On the other hand, images recorded at 35 °C (Fig. 2c) exhibit mainly the presence of short almost round aggregates that cover only 13% of mica surface. Of course, AFM does not allow for fully understanding the underlying mechanism. Still, the reported behaviour seems to suggest that two concurring processes are active.

In general, the thermodynamic parameters, $\Delta H_{\text{disaggr}}$ and cac , associated with the disaggregation of surfactant, biological detergents and polymers, can be successfully obtained by ITC [18, 19].

To this purpose, the 1.9 mM solution was also utilized as titrant in ITC experiments carried out at the three different temperatures. In our experiments all concentrated peptide solutions were utilized 2 h after preparation to be sure that the aggregation was almost complete [11], while the disaggregation is supposed to be fast enough as compared to ITC time scale.

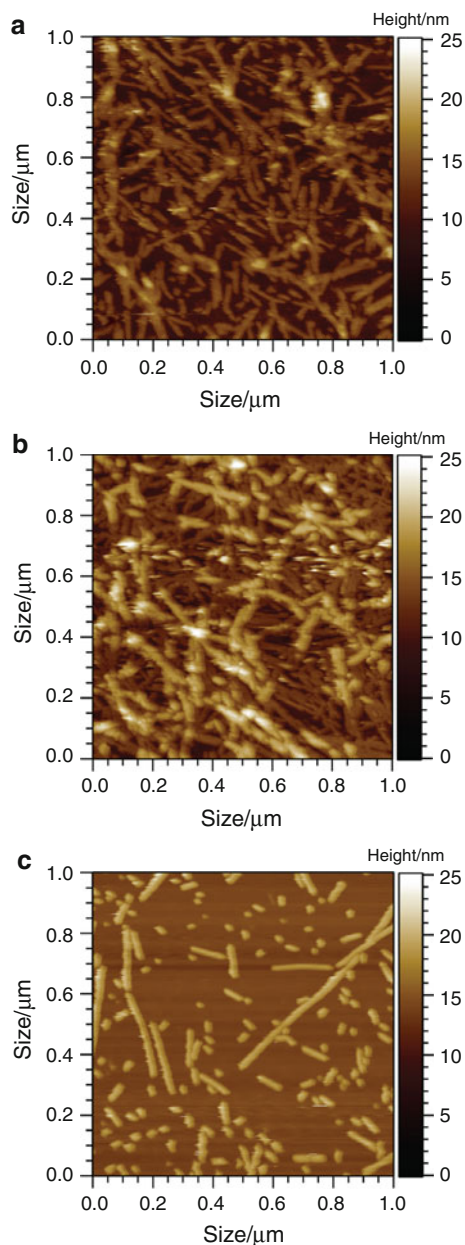
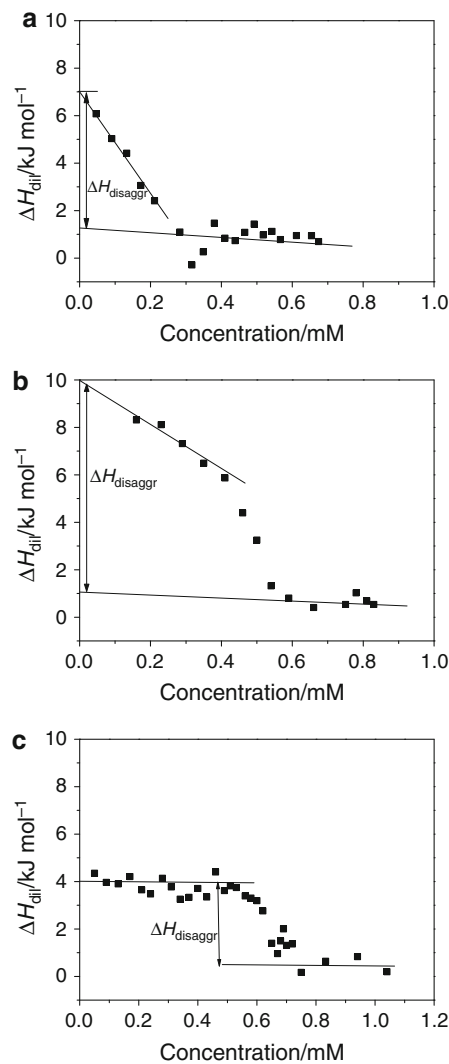
The titrations consisted of sequential additions of the 1.9 mM oligopeptide solution to a PB50 solution contained in the calorimetric cell. The heat effect of each addition is endothermic and in general quite small thus making peak integration rather difficult. On increasing the oligopeptide concentration in the sample cell, in all experiments the heat flow decreases and tends to become constant (almost zero) at the end of the experiment. The experimental design of the ITC investigation implies the disaggregation of supramolecular structures since they are being diluted by the buffer in the calorimetric cell. Of course aggregate disruption gives rise to an increase in oligopeptide concentration. In the first part of the titration the overall enthalpic effect (ΔH_{dil}) results from three phenomena: the dilution of the aggregates, the break down of the aggregates and the dilution of the monomeric oligopeptide. When the cac is reached the heat effect of disaggregation vanishes and the enthalpic effect of aggregate dilution only persists in the last part of the titration (beyond the cac).

Curves recorded at 25 and 35 °C show a sigmoidal feature, while titrations performed at 15 °C generate enthalpograms that do not present such a behaviour (Fig. 3). In fact, at 15 °C we observe a steady decrease in the ΔH_{dil} to up to a certain extent (around 3 mM) after which the enthalpic effect is almost constant (Fig. 3a). At 25 °C the first part of the

Table 1 Average characteristics of RWDW aggregates as evaluated by AFM topographic measurements

Temp./°C	Contact time/s	Number of fibrils	Coverage/%	Circularity	L/nm	W/nm	H/nm
15	20	78	28	4.3	53	22	4.8
25	20	100	27	6.2	124	22	5.2
35	20	116	28	3.4	89	25	6.0
15	300	nd	44	5.8	nd	30	5–6
25	300	nd	98	3.4	nd	35	5–10
35	300	173	13	2.2	21	35	5–6

Coverage is the average per cent of mica surface covered by aggregates; circularity is the ratio of the square of perimeter to $(4\pi \cdot \text{object area})$, approaches 1 for perfect circle; L , W and H are the average length, width and height of aggregates; nd means not determined

**Fig. 2** AFM topographic image of RWDW 1.9 mM solution in PB50 cast on mica after 300 s contact time: **a** 15 °C, **b** 25 °C and **c** 35 °C**Fig. 3** Typical dilution enthalpogram of RWDW in phosphate buffer solution (50 mM, pH 3.5) performed at 15 °C (**a**), 25 °C (**b**) and 35 °C (**c**)

enthalpogram shows a descending trend before the attainment of the inflection point (Fig. 3b), whereas at 35 °C the ΔH_{dil} in the first part of the curve is almost constant (Fig. 3c).

In a previous article we reported a value of 4.9 ± 0.5 kJ mol⁻¹ for the $\Delta H_{\text{disaggr}}$ at 25 °C obtained according to the method conventionally reported for sigmoidal curves [19] which basically corresponds to calculate the $\Delta H_{\text{disaggr}}$ at the cac. In this study, where the enthalpograms obtained at 15 °C did not show a sigmoidal behaviour, in order to better compare the $\Delta H_{\text{disaggr}}$ at the three considered temperatures, we decided to calculate the enthalpy of disaggregation at infinite dilution. $\Delta H_{\text{disaggr}}$ was evaluated by a data treatment analogous to that suggested by Klijn et al. [20]. Linear fits of the dataset in the lower and upper concentration ranges were performed and the intercepts of the two straight lines were determined. The enthalpy of disaggregation was then calculated as the difference between the two intercepts (Fig. 3). This procedure corresponds to the ideal process of diluting a concentrated solution containing peptide aggregates to $c = 0$ and breaking the aggregates at infinite dilution. It is noteworthy that at 35 °C, where the heat effects related to the dilution of both the monomeric peptide and supramolecular aggregates seem to be negligible, the $\Delta H_{\text{disaggr}}$ parameters at infinite dilution and at cac coincide.

The cac at 25 and 35 °C was evaluated at the inflection point of the sigmoid. On the other hand the value at 15 °C was estimated as the intersection of the two straight lines singled out by the initial and final points. Because of the high dispersion of the points around the cac, owing to the small heat effects as well as to a slow kinetics of aggregation at this temperature, the cac threshold cannot be singled out neatly. However, the reproducibility of the results encourages us to consider the estimated cac value reliable.

$\Delta H_{\text{disaggr}}$ and cac values determined by ITC at different temperatures are reported in Table 2.

We can observe that in all cases the disaggregation process is endothermic showing that the self-assembly of the RWDW oligopeptide is enthalpically favoured. Table 2 also shows that the cac increases with increasing temperature. This behaviour is consistent with the positive value of $\Delta H_{\text{disaggr}}$. Otherwise, the dependence of $\Delta H_{\text{disaggr}}$ on temperature does not show a well-defined trend in the observed range. On the other hand, depending on the experiment temperature the disaggregation process affects aggregates having three distinct morphologies, as clearly

Table 2 Comparison of cac and $\Delta H_{\text{disaggr}}$ as determined at different temperatures

$T/^\circ\text{C}$	cac/mM	$\Delta H_{\text{disaggr}}/\text{kJ mol}^{-1}$
15	0.3 ± 0.05	5.7 ± 0.6
25	0.5 ± 0.04	8.9 ± 0.7
35	0.6 ± 0.05	3.5 ± 0.5

shown by AFM measurements. Differences in the aggregation enthalpy at different temperatures may be related to differences in the number of oligopeptides molecules involved in the formation of supramolecular aggregates. Actually, AFM topographic images of RWDW solution 1.9 mM at 35 °C show the presence of well-separated fibres arranged in a much simpler array than at 15 and 25 °C.

To further clarify this point DSC scans of RWDW solutions were performed at different concentrations (close to and above the cac of the system prepared at 25 °C). The DSC scans confirm that the RWDW aggregation is a rather complex phenomenon. The heating of the most concentrated solution (the same used as titrant in the ITC experiments) showed three peaks below 50 °C and a pronounced peak around 75 °C. Decreasing the concentration led to the progressive disappearance of the peaks below 50 °C (Fig. 4) and to the shift of the peak at 75 °C towards lower temperatures. Heating-cooling cycles showed that the process is not reversible. Very likely degradative processes take place at higher temperature thus preventing the peptide reaggregation.

However, we can observe that the ΔH values measured for the highest temperature peak at different concentrations (Table 3) are almost independent of concentration, within the experimental error, suggesting that they refer to the same process.

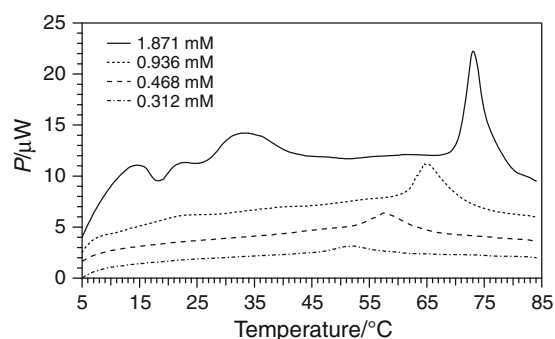


Fig. 4 DSC curves for RWDW solution with different concentration in PB50

Table 3 DSC data of RWDW solutions at different concentrations

RWDW/mM	Peak area/ μJ	$\Delta H/\text{kJ mol}^{-1}$	$T_{\text{max}}/^\circ\text{C}$
0.312	347	3.5	51.9
0.468	547	3.7	57.6
0.936	1045	3.7	65.2 ^a
1.871	2280	3.8	73.1 ^b

^a Smaller peaks are also present at about 22 and 34 °C

^b Smaller peaks are also present at 14, 22 and 34 °C

Of course DSC and ITC data are not directly comparable as they refer to different processes. Yet it is worth noting that the measured ΔH value is in close agreement with the $\Delta H_{\text{disaggr}}$ obtained by ITC at 35 °C.

Conclusions

The reported results indicate that the self-assembly of RWDW is strongly affected by the temperature. Indeed, AFM imaging above the *cac* clearly shows the presence of fibrillar structures that are dense and entangled at 15 and 25 °C, whereas they are few and far between at 35 °C. Moreover, the images at 25 °C reveals overlying layers of fibres.

The different aggregate morphology observed by AFM is in agreement with the observed behaviour by ITC. The combined use of AFM, ITC and DSC allows us to conclude that both the aggregates morphology and the disaggregation process are different at the three temperatures investigated.

Acknowledgements The authors are grateful to the reviewer for helpful suggestions. The financial support by MIUR, INSTM and Fondazione Cassa di Risparmio di Pisa is gratefully acknowledged.

References

- Zhang S. Emerging biological materials through molecular self-assembly. *Biotechnol Adv.* 2002;20:321–39.
- Reches M, Gazit E. Rigid, self-assembled hydrogel composed of a modified aromatic dipeptide. *Curr Nanosci.* 2006;2:105–11.
- Lomakin A, Teplow DB, Kirschner DA, Benedek GB. Kinetic theory of fibrillogenesis of amyloid β -protein. *Proc Natl Acad Sci USA.* 1997;94:7942–7.
- Dobson CM. Protein folding and its links with human disease. *Biochem Soc Symp.* 2001;68:1–26.
- Yu L, Ding J. Injectable hydrogels as unique biomedical materials. *Chem Soc Rev.* 2008;37:1473–81.
- Holmes TC, de Lacalle S, Su X, Liu G, Rich A, Zhang S. Extensive neurite outgrowth and active synapse formation on self-assembling peptide scaffolds. *Proc Natl Acad Sci USA.* 2000;97:6728–33.
- Deming TJ. Synthetic polypeptides for biomedical applications. *Prog Polym Sci.* 2007;32:858–75.
- Hosseinkhani H, Hosseinkhani M, Kobayashi H. Design of tissue-engineered nanoscaffold through self-assembly of peptide amphiphile. *J Bioact Compat Polym.* 2006;21:277–96.
- Zhang S, Holmes TC, Lockshin C, Rich A. Spontaneous assembly of a self-complementary oligopeptide to form a stable macroscopic membrane. *Proc Natl Acad Sci USA.* 1993;90:3334–8.
- Desii A, Chiellini F, Duce C, Ghezzi L, Monti S, Solaro R, Tiné MR. Influence of structural features on the self-assembly of short ionic oligopeptide. *J Polym Sci Part A: Polym Chem.* 2010;48:889–97.
- Desii A, Duce C, Ghezzi L, Monti S, Solaro R, Tiné MR. Investigation of the self-assembly of hydrophobic self-complementary ionic tetrapeptides. *J Therm Anal Cal.* 2009;97:789–90.
- Desii A, Chiellini F, Di Stefano R, Tiné MR, Solaro R. Hydrogel scaffolds by self-Assembly of a complementary ionic tetrapeptide. *J Polym Sci Part A: Polym Chem.* 2010;48:986–90.
- Pochan DJ, Schneider JP, Kretsinger J, Ozbas B, Rajagopal K, Haines L. Thermally reversible hydrogels via intramolecular folding and consequent self-assembly of a de novo designed peptide. *J Am Chem Soc.* 2003;125(39):11802–3.
- Jeong B, Bae YH, Lee DS, Kim SW. Biodegradable block copolymers as injectable drug-delivery systems. *Nature.* 1997;388:860–2.
- Privalov PL. Stability of protein-structure and hydrophobic interactions. *Biol Chem Hoppe Seyler.* 1988;369:199.
- Ye Z, Zhang H, Luo H, Wang S, Zhou Q, DU X, Tang C, Chen L, Liu J, Shi YK, Zhang EY, Ellis-Behnke R, Zhao X. Temperature and pH effects on biophysical and morphological properties of self-assembling peptide RADA16-I. *J Pept Sci.* 2008;14:152–62.
- Ramachandran S, Taraban MB, Trehwella J, Gryczynski I, Gryczynski Z, Yu YB. Effect of temperature during assembly on the structure and mechanical properties of peptide-based materials. *Biomacromolecules.* 2010;11:1502–6.
- Garidel P, Hildebrand A. Thermodynamic properties of association colloids. *J Therm Anal Cal.* 2005;82:483–9.
- Majhi RP, Blume A. Thermodynamic characterization of temperature-induced micellization and demicellization of detergents studied by differential scanning calorimetry. *Langmuir.* 2001;17:3844–51.
- Kljin JE, Kevelam J, Engberts JBFN. Aggregation behavior of mono-encapped hydrophobically modified poly(sodium acrylate)s in aqueous solution. *J Coll Interf Sci.* 2000;226:76–82.